

Andrea Berlich · Beate Flemmig · Gunther Wittstock

Formation of polymer-modified electrodes from 2-mercaptobenzoxazole in aqueous solution

Received: 7 September 2000 / Accepted: 7 November 2000 / Published online: 14 June 2001
© Springer-Verlag 2001

Abstract A polymer-modified electrode can be formed from 2-mercaptobenzoxazole (MBO) on glassy carbon (GC) electrodes in aqueous solution. Film formation occurs during prolonged cycling with positive scan limits above +600 mV vs. SCE. The main redox process is the oxidation of MBO to bis(benzoxazolyl) disulfide and the re-reduction to MBO. However, several side reactions including polymerization are observed. A density functional calculation of the MBO radical shows that there is a considerable spin density not only at the sulfur atom but also at the nitrogen atom and at some of the carbon atoms. Therefore ring-ring coupling products other than the disulfide can be formed which may further react to the polymer film. Notably, FTIR spectra indicate substitution at the nitrogen atom. The coupling would explain the occurrence of both thione and bridging sulfur as well as amine and imine nitrogen in the formed polymer. These binding states in the film have been identified by X-ray photoelectron spectroscopy (XPS). Elemental sulfur could not be detected by cyclic voltammetry or XPS of cooled samples. The polymer film is not redox active and non-conducting, as illustrated by the self-limiting growth and the diminishing currents during the potentiodynamic film growth. The film is impermeable for anions. At pH 7 the film is permeable for cations, while it is impermeable for anions and cations at pH 4.

Keywords 2-Mercaptobenzoxazole · Polymer-modified electrodes · Density functional calculation · X-ray photoelectron spectroscopy · Polymerization

Introduction

The electrochemistry of 2-mercaptobenzoxazole (MBO) and 2-mercaptobenzothiazole (MBT) has been studied in the past for their determination in rubber, where they are used as accelerators in the vulcanization process [1, 2], or their application as complexing agents in the trace determination of heavy metals [3, 4], in the separation process of sulfide ores using flotation [5], or as corrosion inhibitors [6], as well as in electrosynthesis [7, 8].

In a preceding communication [9] about the oxidation of MBO in aqueous solution, it was demonstrated that the oxidation and reduction processes occurring between –1200 mV and +800 mV (vs. SCE) are dominated by the formation of bis(benzoxazolyl) disulfide (BBOD). Owing to its extremely low solubility, oxidation products remain at the electrode surface, where they form microcrystals if the BBOD surface concentration exceeds about three monolayers. The formation of microcrystals instead of an adsorbed layer alters the appearance of the cyclic voltammograms (CVs).

CVs with a more positive potential excursion (–1200 mV to +1300 mV) revealed four anodic signals (denoted Ia–IVa in Fig. 1) and two cathodic signals (IIc and IIIc). The anodic signals that also occur during voltammetric cycling of the related compounds MBT and 2-mercaptobenzimidazole (MBI) have been formerly assigned to the formation of sulfonic acids [10] or the formation of a polymer film [11] from MBT and MBI. While the film formation could be demonstrated, no conclusions about its chemical nature were attempted [11]. Therefore, in this study we determined structural motives and properties of a polymer film obtained from prolonged cycling of a glassy carbon (GC) electrode in aqueous MBO solution for the first time. The results are compared with quantum mechanical computations to explain the mechanism of polymer formation. Furthermore, the dependence of the anodic and cathodic peak potentials on the pH value has been evaluated.

A. Berlich · B. Flemmig · G. Wittstock (✉)
Wilhelm Ostwald Institute of Physical and
Theoretical Chemistry,
University of Leipzig, Linnéstrasse 2,
04103 Leipzig, Germany
E-mail: wittstoc@rz.uni-leipzig.de
Fax: +49-0341-9736399

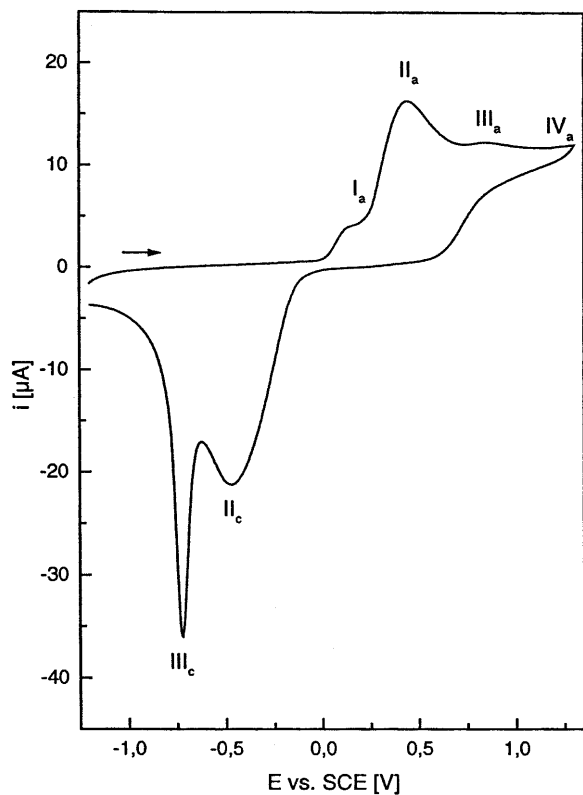
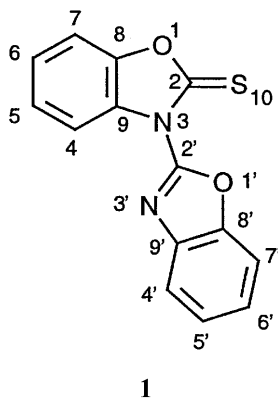


Fig. 1 Cyclic voltammogram (CV) of a GC electrode in 3 mM MBO solution (phosphate buffer, pH 7.0, $\nu = 25 \text{ mV s}^{-1}$). Peaks are labelled with Roman numbers

Experimental

[Ru(NH₃)₆]Cl₃ (Strem, Kehl, Germany) and K₄[Fe(CN)₆] (Merck, Darmstadt, Germany) were used as received. MBO (95%, Aldrich, Steinheim, Germany) was recrystallized from ethanol. BBOD was synthesized by oxidation of MBO with H₂O₂ in glacial acetic acid and recrystallized from ethanol/water [12]. The compounds were characterized by elemental analysis, ¹H and ¹³C NMR, mass spectrometry and their melting points. The analytical results are given in supplementary material published previously [9].

An attempt was made to synthesize the bis(benzoxazolyl) monosulfide (BBOM) from the sodium salt of MBO and 2-chlorobenzoxazole in dimethylformamide at 410 K, similar to a published procedure [13] for the related compound bis(benzothiazolyl) monosulfide. However, 3-(1,3-benzoxazol-2-yl)-1,3-benzoxazole-2-thione (BOBOT, Structure 1) was obtained instead with 70% yield



and characterized by melting point (156–157 °C, corrected); elemental analysis for C₁₄H₈N₂O₂S: C 62.6% found (62.7% calc.), H 3.2% (3.0%), N 10.1% (10.4%), O 12.2% (11.9), S 11.4% (11.9%); ¹H NMR (200 MHz) in ppm: 7.35, 7.43 (multiplet (m) overlapping for 5H, 6H, 5'H, 6'H), 7.66 (m, overlapping, for 7H, 7'H), 7.80, 7.89 (m for 4H, 4'H); ¹³C NMR (¹H decoupled) in ppm, protonated: 110.8, 111.6, 113.7, 120.8 (C4, C4', C7, C7'), 126.0, 126.6, 126.5 (C5, C5', C6, C6'); non-protonated: 130.4 (C9), 140.5 (C9'), 147.5 (C2'), 149.6 (C8), 151.4 (C8'), 177.2 (C2). The ¹³C NMR signal at 177.2 indicates the conservation of the -N-C=S group. For the -N=C-S- group a considerable negative shift would be expected (for example, in BBOD to 159.9 ppm). The signal of carbon atom C2' at 147.5 ppm shows that the second ring system does not contain an equivalent group. MS data: *m/z* 268 (100% *M*⁺), 210 (41%, [*M*-NCS]⁺), 208 (58%, [*M*-OCS]⁺), 179 (80% [*R'*(COH)S]⁺), 153 (30%), 134 (13%), 122 (15%), 90 (80%), 78 (29%), 64 (56%), 63 (73%), 50 (49%), 38 (60%). The absence of signals at 150 and 118 for [*R'*]⁺ and [*R'-S*]⁺, respectively, proves that the molecule does not contain a *R'-S-R* bridge between the two ring systems. The [*R'-S*]⁺ and [*R'*]⁺ signals are very intense in bis(benzothiazolyl) monosulfide, which was synthesized according to the published procedure [13]. X-ray photoelectron spectroscopy (XPS) binding energy shifts further prove the structural assignment and will be discussed later.

Other chemicals, instruments and procedures are the same as described previously [9]. All electrochemical potentials are given with respect to the saturated calomel electrode (SCE). Atomic ratios from XPS intensities were calculated using atomic sensitivity factors [14].

For the MBO radical a complete geometry optimization was performed using density functional theory in the unrestricted formalism (UDFT). Subsequent to this calculation the total atomic spin densities were obtained with a Mulliken population analysis. The B3LYP functional [15, 16] and the 6-31G* basis set were applied in the calculation that was carried out with the GAUSSIAN 94 package [17].

Results and discussion

Voltammetric signals of MBO

A typical cyclic voltammogram of a GC electrode in MBO solution is given in Fig. 1. Four anodic and two

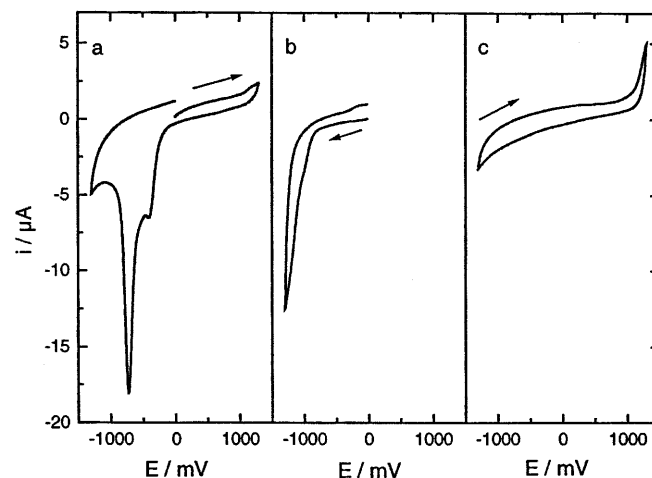


Fig. 2 CVs of substances deposited on a rotating GC electrode: **a** 5 μL 10 mM BBOD in CHCl₃, **b** 5 μL 10 mM elemental sulfur in CHCl₃, **c** 5 μL 10 mM BOBOT in CHCl₃. CVs were recorded in phosphate buffer, pH 7, at 25 mV s^{-1}

cathodic processes are observed. Anodic processes I_a and II_a were assigned to the $1H^+, 1e^-$ oxidation of adsorbed and dissolved MBO [9], leading to the formation of its disulfide after dimerization. The nature of the

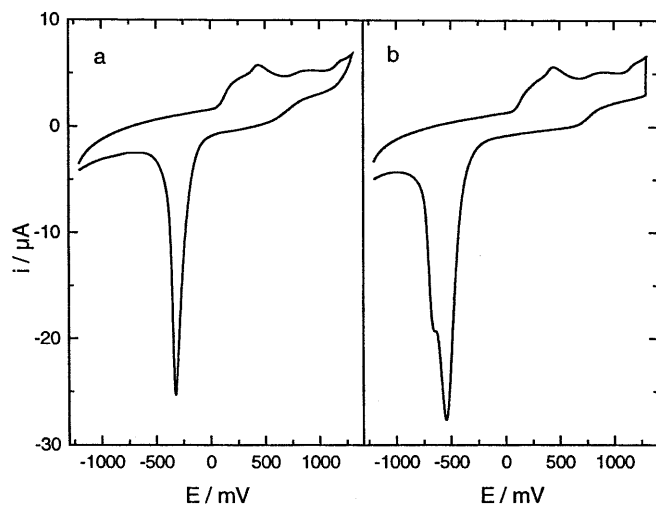


Fig. 3 CVs of MBO at 25 mV s^{-1} at high concentrations or after constant-potential electrolysis: **a** 1 mM MBO between -1200 mV and $+1300 \text{ mV}$, **b** 1 mM MBO between -1200 mV and $+1300 \text{ mV}$ with 2 min electrolysis at $+1300 \text{ mV}$

anodic processes responsible for signals III_a and IV_a is less clear. They can be caused by further oxidation of BBOD (vide infra). Direct oxidation of MBO to the corresponding sulfonic acid has been reported at Pt electrodes and might contribute to the overlapping signals at $E > 0.8 \text{ V}$ as well [10].

In the following negative half-cycle, two cathodic peaks (II_c and III_c) are observed. These peaks are found if all of the following conditions are met: (1) the positive potential excursion exceeds $+600 \text{ mV}$; (2) the MBO bulk concentration is above 1 mM ; (3) the scan rate is not too high, i.e. for a 3 mM MBO solution the double peak is observed for scan rates up to 100 mV/s . To attempt an assignment of the redox signals II_c and III_c , several suspected oxidation reaction products were transferred to the GC electrode by solvent evaporation on a rotating electrode. The electrode was transferred to plain buffer and a cyclic voltammogram was recorded (Fig. 2). If chemically synthesized BBOD as the major oxidation product up to $+600 \text{ mV}$ is deposited onto the electrode, and the amount exceeds a critical value, a characteristic double peak is found similar to the signal obtained (Fig. 2a) in the negative-going half-cycle of a CV of MBO (Fig. 1). A single reduction signal is obtained if much less BBOD is deposited onto the GC electrode (fig. 8 of [9]). The amount of electrochemically formed BBOD can be increased systematically by either

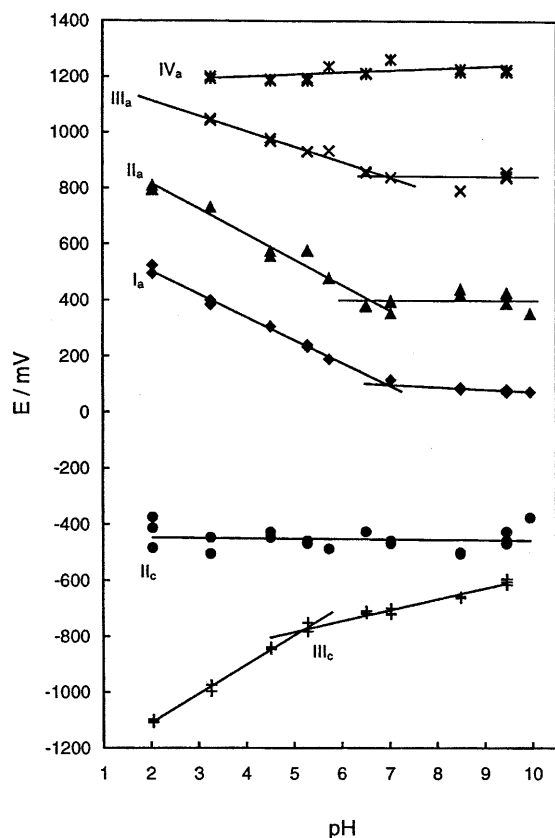


Fig. 4 Dependence of signals in CVs of MBO on pH; $c(\text{MBO}) = 3 \text{ mM}$, $v = 25 \text{ mV s}^{-1}$, scans between -1200 mV and $+1300 \text{ mV}$

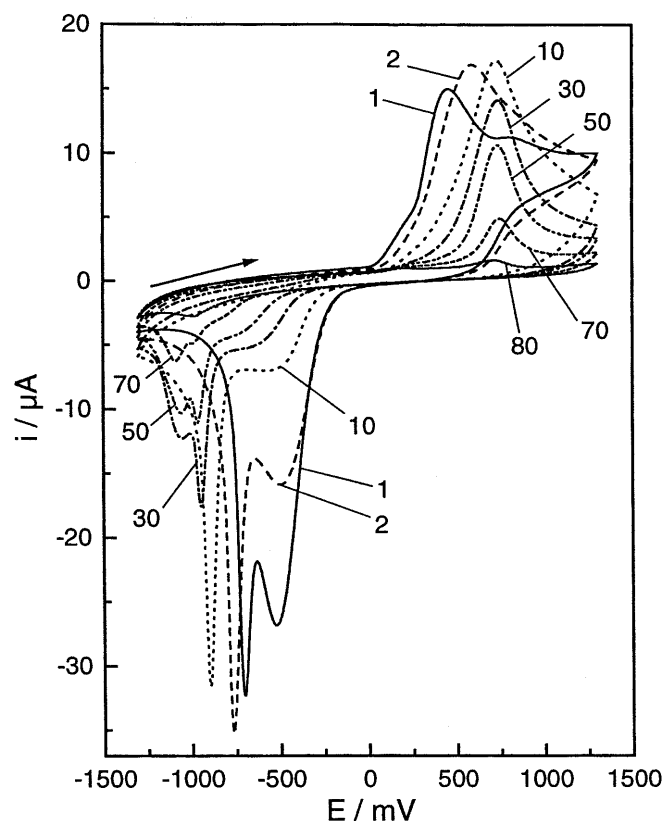


Fig. 5 Selected cycles out of 80 consecutive CVs in a solution of 3 mM MBO, $\text{pH } 7.0$, $v = 25 \text{ mV s}^{-1}$. Numbers indicate the cycle number

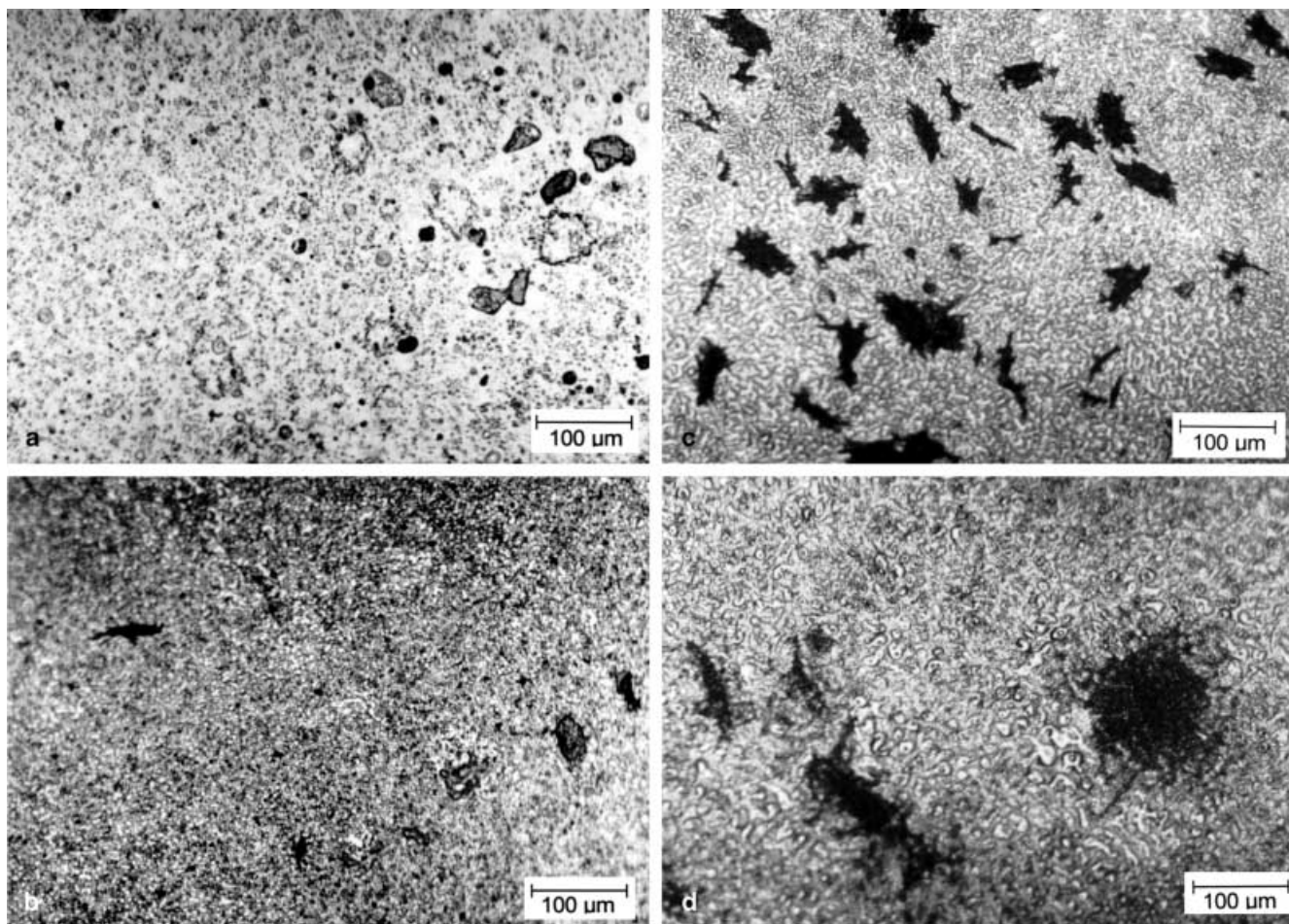


Fig. 6a–d Interference microscope pictures showing film formation during redox cycling between -1200 mV and $+1300$ mV with 25 mV s^{-1} in a 3 mM MBO solution, pH 7. Immersion of the electrode was carried out at -1200 mV **a** after the first complete cycle, **b** after 5 cycles, **c** after 15 cycles and **d** after 80 cycles

increasing the MBO bulk concentration, the anodic vertex potential E_{λ} , or inserting a constant-potential electrolysis time at E_{λ} . Under such circumstances the cathodic signal III_c grows, depending on the amount of BBOD formed (Fig. 3). At constant solution concentration, signal III_c becomes more dominant over signal II_c as the time frame of the experiment is increased either by lowering the scan rate or by inserting a constant potential electrolysis between the positive and negative half-cycles (Fig. 3). Note that this observation is only made if the anodic potential excursion extends beyond $+600$ mV.

The small oxidation signal at $+1200$ mV in the CV of deposited BBOD (Fig. 2a) as well as of MBO oxidation (Fig. 1) may be associated with the formation of sulfonic acids, which have been suggested as oxidation products at high positive potentials [10]. The 1,3-benzoxazole-2-sulfonic acid has a much better solubility in aqueous solution than MBO and is expected to diffuse away from the electrode. Other compounds with $-SOH$ or $-SO_2H$

groups formed from MBO directly or via the disulfide are expected to have similar properties.

Elemental sulfur was suggested [7] as a possible oxidation product of the related compound MBT in acetonitrile. Sulfur microcrystals deposited onto a GC electrode by solvent evaporation cause a reduction signal at potentials more negative than -850 mV at pH 7 (Fig. 2b). Because this signal is not found in the CVs of MBO solutions or deposited BBOD, and elemental sulfur could not be detected by XPS, it is concluded that this mechanism is not important for MBO under our experimental conditions.

BOBOT was found as the unexpected reaction product in an attempt to synthesize the 2,2'-bis(benzoxazolyl) monosulfide (BBOM) according to a published procedure [13]. If performed with MBT as the starting material, this procedure yields indeed the expected 2,2'-bis(benzothiazolyl) monosulfide (BBTM). In the case of MBO, however, a detailed structural investigation (see Experimental), which was not carried out in [13], proves the structure of the reaction product to be the one shown in **1**. XPS spectra of BOBOT and BBTM powders confirm that assignment. BOBOT has two N 1s components of equal intensity at 398.4 eV ($=N^-$) and 400.7 eV ($-N<$) and one S $2p_{3/2}$ component at 161.4 eV which corresponds to the exocyclic sulfur in the thione

form (=S). In contrast, BBTM has one N 1s component only at 398.6 eV (=N-). The S 2p signals of the endocyclic sulfur atom and the exocyclic bridging sulfur in BBTM cannot be distinguished by their chemical shift in XPS. Both contribute to the S 2p_{3/2} emission at 164.0 eV (-S-). If BOBOT is transferred to the GC electrode by solvent evaporation and reduced in aqueous buffer, a reduction current at potentials negative of -200 mV is recorded (Fig. 2c). However, no clear peak is visible, possibly indicating a very slow overall reaction mechanism.

The signals I_a-IV_a and II_c and III_c show a very remarkable and not yet fully understood pH dependence (Fig. 4). The oxidation processes show a dependence of -77 up to -90 mV/pH, in accordance with the proposed 1H⁺, 1e⁻ processes leading to the MBO radical. The pK_S of MBO is 7.3. In agreement, the peak potential for the MBO oxidation is pH independent at pH > 7. Values reported by Goyal and Verma [18] have the same slope but the absolute values are between those of our signals I_a and II_a. The experimental conditions in [18], however, were slightly different: c(MBO) = 0.5 mM, ν = 10 mV s⁻¹, pyrolytic graphite electrode. The change of slope for pH < 4 reported in [18] is not confirmed by our data. The peak potential of signal III_a follows the same trend as those of I_a and II_a. The slope for pH < 7 is -55 mV/pH. Signal IV_a has a pH-independent peak potential, although it should be noted that the determination of this peak potential is very difficult owing to the overlap of the various signals in the potential region. The reduction process II_c is independent of pH at high MBO concentration. If the concentration is decreased to 0.5 mM a slope of -29 mV/pH is found, which is similar to the results of Goyal and Verma [18] who reported -40 mV/pH for this signal. A rather unusual *positive* pH shift of +105 mV/pH (pH < 5.1) and +39 mV (pH > 5.1) is obtained for signal III_c. As reductions of organic compounds are usually an overall uptake of protons and electrons, this behavior is remarkable. A positive pH dependence was reported by Bond et al. [19] for the reduction of indigo microcrystals. The authors explained the phenomenon by sodium ion uptake, which is inhibited at high proton concentrations. In our study, however, the effect is much stronger than in [19] and at the moment not understood.

Polymer formation

During a multi-cycle voltammogram the anodic peaks lose the signature of the MBO oxidation (Fig. 5). Instead of the four overlapping signals in the first cycle, one signal for surface-confined redox species at +750 mV is observed from the 30th cycle on. In subsequent cycles the reduction peak at -500 mV decreases and correspondingly the sharp peak between -700 mV and -830 mV increases and is shifted to more negative potentials. Eventually, a shoulder at even more negative potentials develops after the 30th scan. The total signal

height decreases from cycle to cycle until almost negligible signals are recorded in the 80th scan (vide infra). This is explained by the deposition of a polymer film, which can be seen clearly in a sequence of interference microscopic images shown in Fig. 6. During the positive half-cycle an insoluble product is formed on the electrode surface (compare fig. 10 of [9]). This is almost completely removed during the following negative-going scan. After the first complete cycle, only some deposits remain on the electrode surface (Fig. 6a). These deposits appear to grow upon subsequent cycling (Fig. 6b). As can be seen in Fig. 6c, a rather pronounced inhomogeneity of the film on a scale of some 10 μm is observed. Extensive cycling, however, leads to a dense film covering the entire electrode surface (Fig. 6d). The microscopic pictures suggest that the growth rate of the film is fastest in the early voltammetric cycles.

A plot of the charges transferred in the positive and negative half-cycles (Fig. 7) shows that up to about the 30th cycle there is an excess of anodic charges. As evident from [9], this excess occurs only if the positive switching potential E_s exceeds +800 mV. The equal anodic and cathodic charges observed from the 30th cycle onwards suggest that these reactions do not contribute to the build-up of the film, but originate from redox-active groups within the film. Because the charge

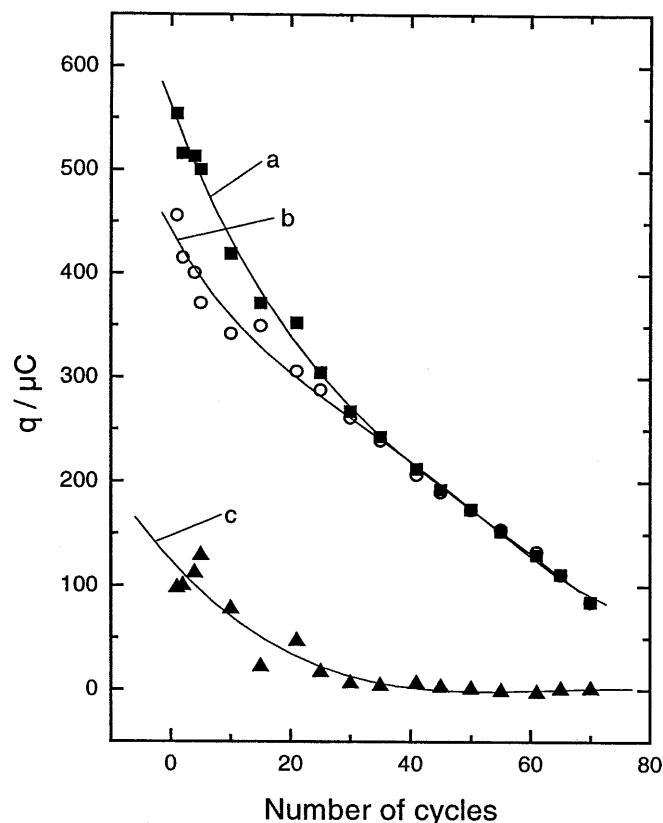


Fig. 7 Charges transferred in each cycle of a multi-cycle CV. Conditions are the same as in Fig. 5: *a* anodic charges, *b* cathodic charges, *c* difference of cathodic and anodic charges

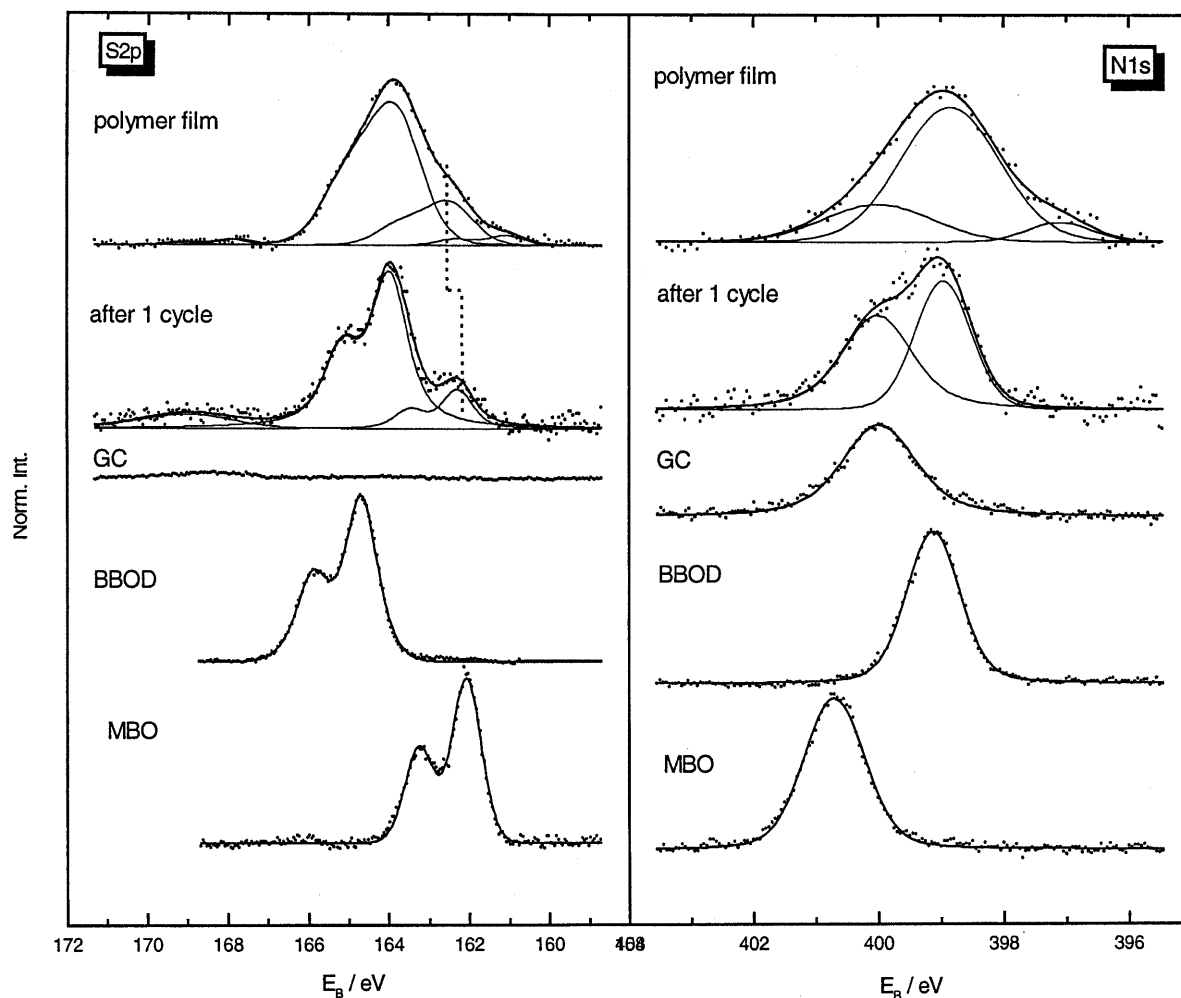


Fig. 8 S 2p and N 1s photoelectron spectra of MBO and BBOD powder and of a GC electrode before and after potentiodynamic treatment in 3 mM MBO solution (pH 4, 25 mV s^{-1} , -1250 to $+1300$ mV) after the first complete cycle and after 80 cycles (polymer film). The polymer film was measured using non-monochromatized Mg K_{α} excitation. All other spectra were obtained using monochromatized Al K_{α} radiation

Table 1 Binding energies and intensities corrected by atomic sensitivity factors of the N 1s and S 2p components in the film formed during 80 potentiodynamic cycles between -1300 mV and $+1300$ mV with 25 mV s^{-1} in 3 mM MBO solution

Signal	Binding energy (eV)	Corrected intensity (%)
S $2p_{3/2}$ (=S)	162.6	0.7
S $2p_{3/2}$ (-S-)	164.1	2.4
N 1s (=N-)	399.2	2.6
N 1s (-N<)	400.3	0.8

per cycle decreases almost linearly with cycle number after the 30th cycle, it can be assumed that these redox-active groups undergo side reactions, eventually leading to a redox-inactive material.

This film formation can also be confirmed using XPS (Fig. 8). GC electrodes immersed after a complete voltammetric cycle between -1250 and $+1300$ mV in

3 mM MBO solution contain some solid deposit left behind after reduction of the BBOD formed during the positive half-cycle. This material has different XPS signals than either BBOD or MBO and is not volatile in UHV. The sublimation behavior in UHV points to a polymeric compound, since many physisorbed organic molecules of medium molecular weight are volatile in UHV. The formation of a monosulfide and elemental sulfur during oxidation as proposed by Chambers et al. [7] for the related compound MBT is unlikely to occur under our experimental conditions because no elemental sulfur could be detected, even when cooling the samples to the temperature of liquid nitrogen. The origin of the small S $2p_{3/2}$ signal at 168.0 eV corresponds to a sulfonic acid group, which may either be formed during sample transfer through air or which might be attached to an insoluble polymer backbone. The intensity ratio of the S $2p_{3/2}$ components at 161.9 eV and 164.2 eV is about 1:3 after the first complete cycle. A quantitative comparison of the N 1s components originating from the material at 399.0 eV and 400.0 eV is not possible, because one of the components overlaps with a N 1s emission from the GC electrode at 400.0 eV. Films formed during 80 cycles in 3 mM MBO solution showed strong charging effects.

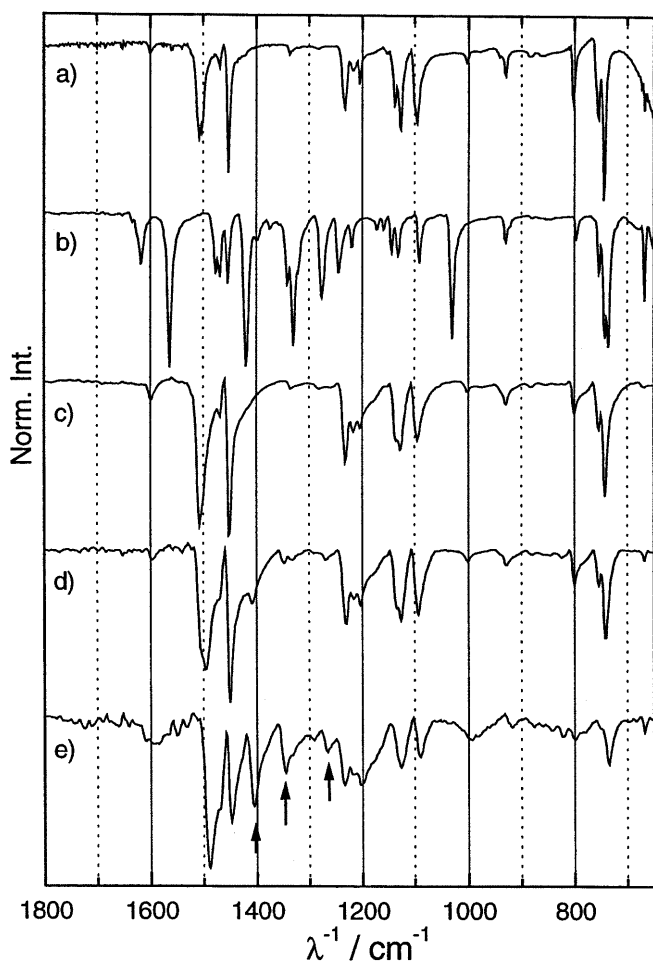


Fig. 9 FTIR spectra of electrochemically deposited products of MBO oxidation and subsequent reductions together with reference spectra of BBOD and BOBOT: **a** BBOD, **b** BOBOT, **c** electrode emersed at +1250 mV after the first half-cycle, **d** electrode emersed at -1250 mV after the first cycle, **e** electrode emersed at -1250 mV after 80 cycles

Therefore, they had to be investigated with non-monochromatized Mg K_{α} excitation, which causes less severe sample charging but does only allow limited spectral resolution (Fig. 8, top spectra). Even with this precaution the C 1s, N 1s, O 1s and S 2p signals of the organic layer showed a component (5–7% of the total line intensity) shifted 2 eV towards lower binding energies. Such an observation is indicative of differential charging. The organic layer directly adjacent to the GC surface is not charged while organic layers on top of this layer exhibit charging versus the conducting GC electrode. The following discussion uses the signals of the multilayer organic film whose binding energies were corrected towards the C 1s binding energy of the overall saturated hydrocarbon contamination at 284.7 eV. The N 1s and S 2p signals have two components each (Table 1). The intensity of signals from the sp^2 -hybridized nitrogen atoms (=N-) at 399.2 eV equals the intensity of emissions from bridging sulfur at 164.1 eV, while the sulfur signal at 162.6 eV corre-

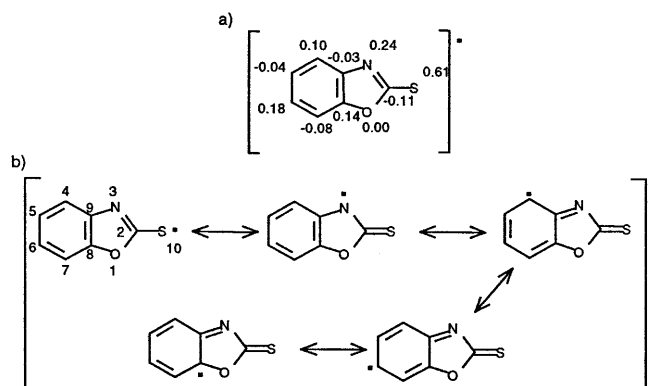


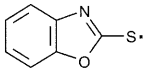
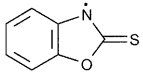
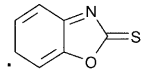
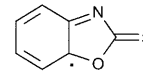
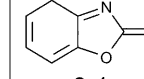
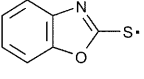
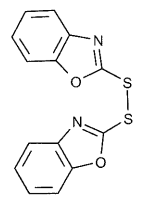
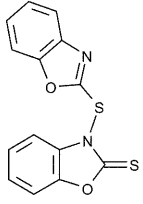
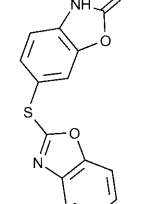
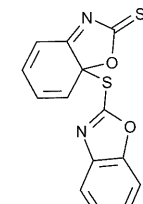
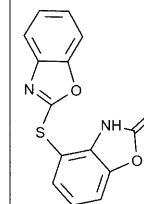
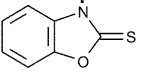
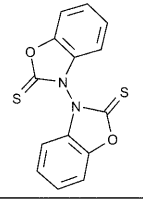
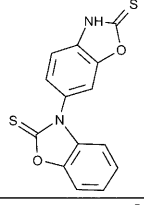
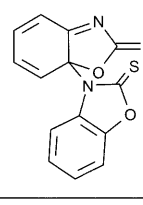
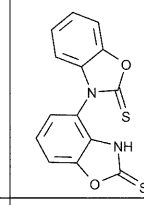
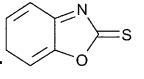
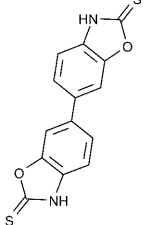
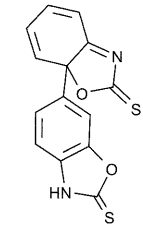
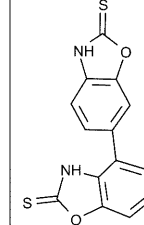
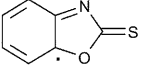
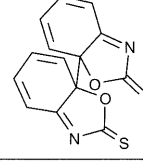
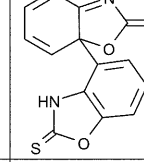
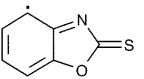
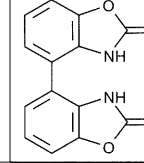
Fig. 10 **a** Calculated atomic spin densities for the MBO radical. **b** Resonance structures of the MBO radical

sponds to that of sp^3 -hybridized nitrogen at 400.2 eV within the accuracy of the method. The intensity ratio between sp^3 and sp^2 nitrogen atoms is 1:3 as well as that between the sulfur with a binding energy of 162.6 eV and bridging sulfur. The S $2p_{3/2}$ binding energy of this signal is 0.7 eV higher than that of the thione sulfur recorded after the first voltammetric cycle (Fig. 8, two topmost spectra).

Further insights for the assignment of the signals come from FTIR spectra of GC electrodes modified with the electrochemically formed polymer film and reference samples (Fig. 9). The spectrum of an electrode emersed at +1250 mV during the first voltammetric cycle corresponds to that of BBOD (Fig. 9a and c). Under these conditions, BBOD is the only oxidation product which remains at the electrode surface at detectable amounts. If other products are formed, they diffuse away (such as sulfonic acids). The spectrum of the electrode emersed at -1250 mV shows three new signals at 1406 cm^{-1} , 1345 cm^{-1} and 1266 cm^{-1} (indicated by arrows, Fig. 9d). Each of the bands corresponds to a band in the spectrum of BOBOT (Fig. 9b). In particular, the band at 1406 cm^{-1} indicates a structural change at the thioamide group. This is caused by a connection of the two rings at the N atom. However, other very intense bands of BOBOT are not found at the modified electrode. Therefore BOBOT itself cannot be the compound deposited at the electrode surface. Continuous cycling leads to an increase of the signals discussed above. No new bands appear. The FTIR spectra confirm that, in the polymer, at least some MBO units are linked via the nitrogen atom.

The first step in MBO oxidation is the formation of a neutral radical. Follow-up reactions of this radical are believed to be dominated by radical-radical recombinations [20]. The main oxidation product is the disulfide formed by dimerization of two radicals. This was proved by the spectroscopic identification and by reduction of chemically synthesized BBOD attached to the electrode surface by solvent evaporation in air and transfer to the electrolyte. However, the MBO radical

Table 2 Possible reaction products by recombination of two MBO radicals. The atomic spin density is given below the corresponding resonance formula of the radical

	 0.61	 0.24	 0.18	 0.14	 0.1
					
					
					
					
					

formed in a $1\text{H}^+, 1\text{e}^-$ oxidation step has significant spin densities at the nitrogen and some carbon atoms that may also lead to other recombination products.

In order to obtain further insight into the characteristics of the MBO radical, DFT calculations in the unrestricted formalism were carried out. The total atomic spin density values are presented in Fig. 10a. They were obtained as the difference of the α and β spin densities. In the calculation, α spin is assigned to the unpaired electron of the radical. Consequently, a high positive value for the atomic spin density corresponds to a high probability of finding the unpaired electron at the corresponding atom. The quantum chemically obtained distribution of the atomic spin densities among the atoms is also reflected by the most relevant resonance structures of this radical, which are depicted in Fig. 10b. In all these structures the unpaired electron is located at the atoms with the highest

calculated spin density (S, N, C4, C6, C8). The strict alternation of positive and negative total spin density values over the molecule indicates a distinct spin polarization starting from the sulfur center and ending between O and C8. This effect can be interpreted by the use of the “intraatomic Hund’s rule”, which postulates that electrons tend to have parallel spins at the same atom.

The considerable spin density at the nitrogen and carbon atoms 4, 6 and 8 should result in a variety of recombination products. Some of the possible recombination products are given in Table 2. Recombination products that link the sulfur atom of one MBO unit with the N, C4 or C6 atom of another unit have indeed a thione sulfur and a sp^3 -hybridized nitrogen. This would explain the occurrence of those signals in the XP spectra. In agreement with the XPS data, bridging S and sp^2 -hybridized N are predicted to occur in an atomic ratio of

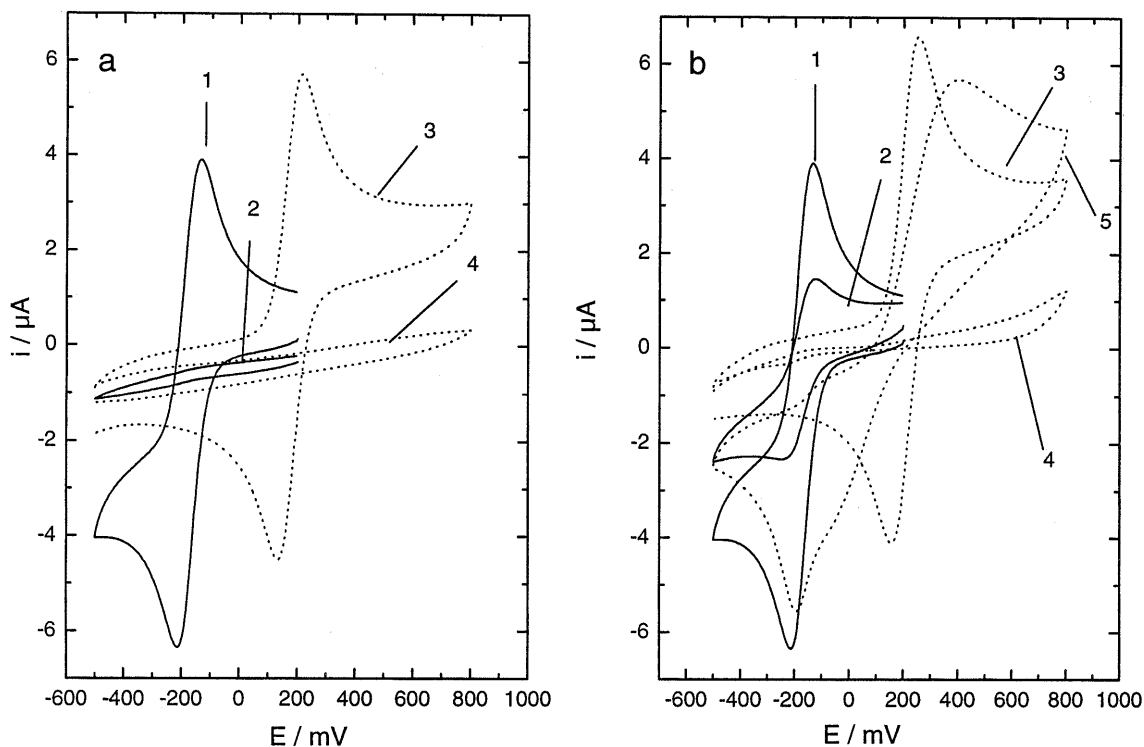


Fig. 11 CV of $[\text{Ru}(\text{NH}_3)_6]^{3+}$ or $[\text{Fe}(\text{CN})_6]^{4-}$ ($c = 1 \text{ mM}$, $\nu = 25 \text{ mV s}^{-1}$) at **a** pH 4, **b** pH 7. Individual curves are 1 $[\text{Ru}(\text{NH}_3)_6]^{3+}$ at a blank GC electrode, 2 $[\text{Ru}(\text{NH}_3)_6]^{3+}$ at a film-covered electrode, 3 $[\text{Fe}(\text{CN})_6]^{4-}$ at a blank GC electrode, 4 $[\text{Fe}(\text{CN})_6]^{4-}$ at a film-covered electrode, 5 $[\text{Fe}(\text{CN})_6]^{4-}$ after rinsing of the film-covered GC electrode with CHCl_3

1:1. The same holds for thione S and sp^3 -hybridized N. The ratio between thione S and bridging S (and between sp^3 to sp^2 N) is 1:3. FTIR spectra also confirmed that rings are linked via N atoms additionally to disulfide bridges between MBO units. Thioketals with a junction via the C8 carbon atom seem to be less stable and are likely to hydrolyze. The compound with a connection at the carbon atoms 6 and 4 can be regarded as substituted MBO molecules, which may form a radical in the same way as MBO itself. The following recombination may be the starting point for forming a stable polymer backbone. The corresponding oxidation signal might be process III_a. The continuous loss of redox activity as shown in Fig. 7 indicates that disulfide bridges may be reduced/re-oxidized until almost all linkages occur via monosulfide bridges and via nitrogen atoms. Such bonds are much harder to convert electrochemically in the investigated potential range.

Because of the variety of possible reaction products and their similar spectroscopic behavior, a more detailed analysis faces considerable difficulties. Some characteristic properties of the film are, however, accessible. The film formed at the GC electrode inhibits heterogeneous redox reactions of dissolved species. $[\text{Ru}(\text{NH}_3)_6]^{3+}$ and $[\text{Fe}(\text{CN})_6]^{4-}$ were selected to probe the inhibiting properties of the film after 80 cycles in MBO solution in dependence on the pH (Fig. 11). At

pH 7 the positively charged $[\text{Ru}(\text{NH}_3)_6]^{3+}$ can still be reduced at the polymer-modified electrode while no oxidation of the negatively charged $[\text{Fe}(\text{CN})_6]^{4-}$ occurs (Fig. 11b, curves 2 and 4). Thus the polymer layer is permeable for cations but not for anions, leading to the conclusion that the polymer contains anionic groups at pH 7 which incorporate cations from solution to maintain electroneutrality. Therefore cations can be transported through the film. Rinsing the film with CHCl_3 dissolves parts of the polymer film and oxidation of $[\text{Fe}(\text{CN})_6]^{4-}$ can be observed after this treatment (Fig. 11, curve 5). At pH 4 the film is impermeable for anions and cations (Fig. 11a, curves 2 and 4). The film is protonated at this pH and ionic species of either charge are not transported.

Conclusions

If the potential excursion during oxidation of MBO exceeds +600 mV, a polymer film is formed at the electrode. This reaction certainly represents a side reaction to the dominating MBO/BBOD redox couple. Therefore a rather high number of potentiodynamic cycles is needed to form polymer films which can be characterized by microscopy, surface spectroscopy and inhibition of probe reactions. MBO units are linked by different structural motives: bridging sulfur and via the nitrogen atoms. During continuous cycling the film loses its redox activity. A self-limiting growth of a non-conducting polymer is observed. The film shows interesting pH-dependent permeabilities for anions and cations. At pH 7 the film contains anionic groups and can

incorporate cations. At pH 4 the film is non-conductive for cations and anions.

Acknowledgements The authors thank V. Gottschalch (University of Leipzig) for providing excess to the interference microscope. FTIR spectra were recorded during a stay of A.B. in the group of G.M. Bancroft (University of Western Ontario) and at Surface Science Western with technical assistance of M.J. Walzac and R. Berno. A.S. received a grant from the German National Merit Foundation. A.B. and B.F. are enrollees of the Graduate Course GRK 152 "Physical Chemistry at Surface and Interfaces" at the Wilhelm Ostwald Institute funded by the Deutsche Forschungsgemeinschaft. Investigation of MBO as a flotation collector was funded by the Deutsche Forschungsgemeinschaft under grant Sz 58/4-1 to R. Szargan. The authors thank R. Szargan and J. Reinhold for discussion on details of this study and for continuous encouragement to pursue this facet of the overall project goals.

References

- Scholz F, Kreutzmann A, Lange B, Dietzsch T, Henrion G (1989) *Z Chem* 29:216
- Fogg AG, Ismail A, Ahmad R, Banica FG (1997) *Talanta* 44:491
- Sousa MF, Bertazzoli R (1996) *Anal Chem* 68:1258
- Khan MM, Khoo SB (1996) *Anal Chem* 68:3290
- Szargan R, Schaufuss A, Rossbach P (1999) *J Electron Spectrosc Relat Phenom* 100:357
- Yan CW, Lin HC, Cao CN (2000) *Electrochim Acta* 45:2815
- Chambers JQ, Moses PR, Shelton RN, Coffen DL (1972) *J Electroanal Chem* 38:245
- Chandrasekaran M, Krishan V (1986) *Transact SAEST* 21:25
- Schaufuss A, Wittstock G (1999) *J Solid State Electrochem* 3:361
- Skacel P, Karlik M, Kucera Z, Dolezal B (1985) *Sci Pap Prague Inst Chem Technol H Anal Chem* 20:31
- Sousa B, de Fatima M, Dallan EJ, Yamaki SB, Bertazzoli R (1997) *Electroanalysis* 9:614
- Arbuzov BA, Zoroastrova (1959) *Izv Akad Nauk Otd Khim* 6:1037
- D'Amico JJ, Webster ST, Campbell RH, Twine CE (1965) *J Org Chem* 30:3618
- Wagner CD, Briggs WM, Davis LE, Moulder JF, Muilenberg GE (1979) *Handbook of X-ray photoelectron spectroscopy*. Perkin Elmer, Eden Prairie, Minn
- Becke AD (1993) *J Chem Phys* 98:5648
- Lee C, Yang W, Parr RG (1988) *Phys Rev B* 37:785
- Frisch MJ, Trucks GW, Schlegel HB, Gill PMW, Johnson BG, Robb MA, Cheeseman JR, Keith T, Petersson GA, Montgomery JA, Raghavachari K, Al-Laham MA, Zakrzewski VG, Ortiz JV, Foresman JB, Cioslowski J, Stefanov BB, Nana-yakkara A, Challacombe M, Peng CY, Ayala PY, Chen W, Wong MW, Andres JL, Replogle ES, Gomperts R, Martin RL, Fox DJ, Binkley JS, Defrees DJ, Baker J, Stewart JP, Head-Gordon M, Gonzalez C, Pople JA (1995) *Gaussian 94* (revision D.4). Gaussian, Pittsburgh
- Goyal RN, Verma MS (1996) *Indian J Chem* 35A:281
- Bond AM, Marken F, Hill E, Compton RG, Hügel H (1997) *J Chem Soc Perkin Trans 2* 1735
- Heinze J, Tschuncky P, Smie A (1998) *J Solid State Electrochem* 2:102